VOL. 11, NO. 5, MARCH 2016 ISSN 1819-6608
ARPN Journal of Engineering and Applied Sciences

www.arpnjournals.com

INVERTED KOCH FRACTAL DUAL BAND DIPOLE ANTENNA WITH HARMONIC SUPPRESSION CAPABILITY

K. B. Suleiman, S. A. Hamzah and A. A. Awaleh
Faculty of Electrical and Electronics Engineering, University Tun Hussien Onn Malaysia (UTHM), Parit Raja, Batu Pahat, Johor, Malaysia
E-Mail: Khaledbensuleiman@gmail.com

ABSTRACT

This paper presents an inverted Koch fractal dual band dipole antenna with harmonic suppression capability. A double-sided Koch fractal dipole antenna incorporated with a tapered balun and operating at 900 MHz and 2.4 GHz was designed. Two rectangular defected ground structures were embedded on the triangular tapered balun to suppress undesired higher-order mode frequencies and enhance antenna performance. Results showed that the antenna functions at the desired frequencies (0.9 and 2.4 GHz) and eliminates higher-order harmonics (3.6 and 4.7 GHz). The antenna was simulated using the electromagnetic simulation software CST Microwave Studio. The simulated and experimental results were compared and good agreement was observed. The proposed antenna design presents a small size and low fabrication complexity.

Keywords: fractal dipole antenna, dual band, harmonic, suppression, inverted Koch.

INTRODUCTION

In the last decade, significant progress in mobile communication systems has improved daily living Antennas are the most significant component of modern communication systems [1]. These devices may be fashioned into different shapes and sizes and implanted in commonly used applications, such as personal communications, home electronics, warfare electronics, and transportation.

Wireless communication systems are generally used as portable or handheld devices. Thus, antennas must be adequately small and compact to fit a device appropriately. Small high-performance antennas are essential in modern communication systems. Such an antenna may reduce the cost and weight of the system device and can be easily embedded in the enclosure of a communication device [2]. In particular, antennas that can operate at more than one frequency are desirable in many modern communication systems.

Various communication systems, including radio frequency identification, wireless broadband systems such as wireless local area networks, and ultra-wideband systems use dipole antennas because of their small size and tenability [3-4]. Several planar fractal dipole antennas have been studied and reported in the literature [5-7]. However, the designs of these antennas present several drawbacks, including large sizes and high fabrication complexity. Besides the Koch curve, numerous fractal geometries have been introduced to different antenna applications to enhance antenna performance and characteristics [8-9]. These fractal patterns include the Minskowski, Sierpinski and Hilbert curves.

Fractal dipole antennas exhibit harmonic frequencies that may corrupt the signal at the operating frequency and affect the resulting quality. To suppress undesirable frequencies, an external filter can be added to eliminate unwanted harmonic frequencies. Various techniques, such as open circuit stubs and split-ring resonators, have been proposed to suppress undesired higher -order modes [10-11].

.

The aim of this paper is to design an inverted Koch dual band fractal dipole antenna with harmonic suppression capability for wireless communications. Two defected ground structures (DGSs) are used to suppress two higher-order modes (second and third harmonics). The dimensions and location of the DGSs are optimized to achieve good performance. The structure of DGS that works best for the particular application could be selected.

ANTENNA DESIGN STRUCTURE

Description of the proposed antenna

Figure-1 illustrates the geometric design structure of the inverted Koch fractal dipole antenna. The antenna is designed to operate at 0.9 and 2.4 GHz. The antenna consists of a transmission line (top layer), triangular tapered balun (bottom layer), and double-sided inverted Koch curve. The inverted Koch curve is employed as a radiating element to reduce the antenna size. A standard Koch curve with a length of 54.9 mm, width of 2 mm, and indentation angle of 60° with two iterations is also used.

The antenna was printed on a standard FR4 substrate with a relative permittivity (ε_r) of 4.3, dielectric loss tangent (tanδ) of 0.019, and substrate thickness of 1.6 mm. The input signal was excited at the bottom end of the top layer transmission line.

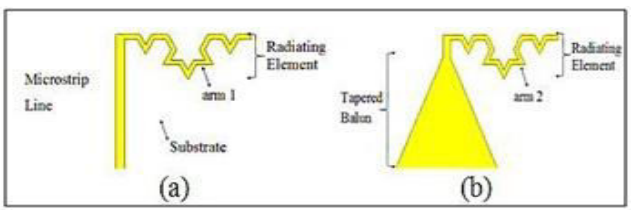

Figure-1. Geometry of the proposed inverted Koch fractal dipole antenna: (a) Top layer and (b) bottom layer.

To determine the overall dimensions of the antenna structure, the following general formulas are used. The microstrip dipole resonance length (L) can be calculated as follows:

$$L = \frac{c}{2f_r\sqrt{\varepsilon_{reff}}} - 2\Delta L \quad (1)$$

Hence, the total length for the second iteration Koch fractal arm is determined using the following equation:

$$L_{koch} = \frac{L}{\left(\frac{4}{3}\right)^2} \quad (2)$$

For the second iteration, the length of each segment is equal to:

$$L_{seq} = \frac{L_{koch}}{9} \quad (3)$$

The proposed inverted Koch fractal dipole antenna is incorporated with two rectangular DGSs to suppress undesired harmonics, as shown in Figure-2. Table-1 summarizes the physical parameters and main features of the optimized antenna.

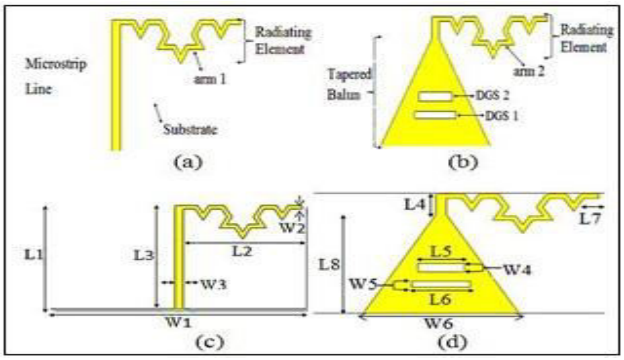

Figure-2. Structure of the inverted Koch fractal dipole antenna incorporated with DGSs: (a, c) Top layer and (b, d) bottom layer.

Table-1. Important design parameters of the antenna.

Dimension	Parameter	Value (mm)
L1	Length of the substrate	119.40
W1	Width of the substrate	58.13
L2	Length of the Koch fractal arm	54.9
W2	Width of the Koch fractal arm	2
L3	Length of the transmission line	58
W3	Width of the transmission line	3.8
L4	Length of the segment from the tapered balun to the arm	8.12
L5	Length of DGS1	21
W4	Width of DGS1	3
L6	Length of DGS2	16.6
W5	Width of DGS2	4
L7	Length of each segment of the Koch arm	6.1
W6	Width of the tapered balun	51

RESULTS AND DISCUSSION

Simulation and measurement results of the antenna without DGSs

The simulated and measured return losses of the antenna before DGS application are shown in Figure-3. In the figure, the antenna operates in the two desired resonant frequencies because the return loss is below –10 dB at frequencies of 900 MHz and 2.4G Hz. Similarly, two undesired frequencies falling below –10 dB are observed. Figure-4 presents the simulated and measured Voltage Standing Wave Ratio (VSWRs) of the antenna without DGSs. Results clearly show a VSWR that is less than 2 at both desired and undesired frequencies.

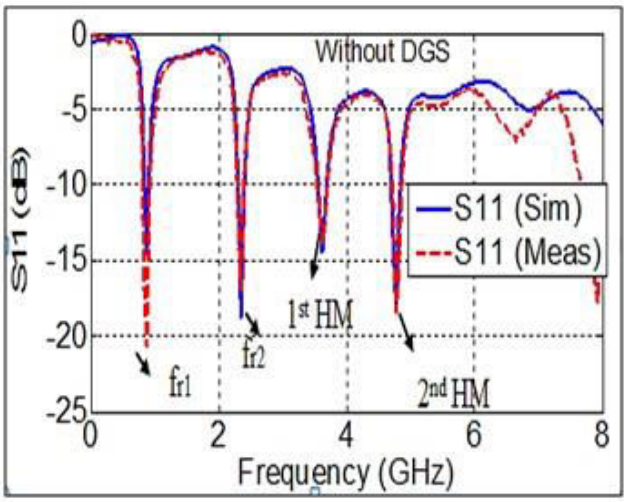

Figure-3. Simulated and measured S11 for the antenna without DGSs.

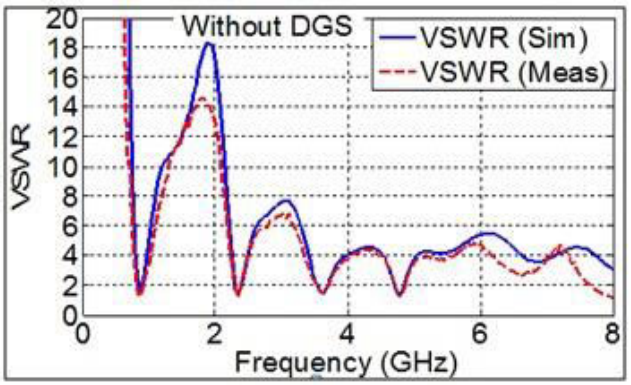

Figure-4. Simulated and measured VSWRs for the antenna without DGSs.

Simulation and measurement results of the antenna with DGSs

Figure-5 shows the effects of DGSs on eliminating the third and fourth undesired frequencies. The DGSs effectively suppress the undesirable frequencies (3.6 and 4.7 GHz) by reducing their amplitudes. As such, the antenna operates at only the two designed resonant frequencies. Both simulated and measured results indicate

a return loss response of approximately –26 dB at 0.9 GHz and –21 dB at 2.4GHz. The effect of the DGSs on the VSWR is shown in Figure-6. The VSWR results of the undesirable frequencies are consistently greater than 16 after application of the DGSs.

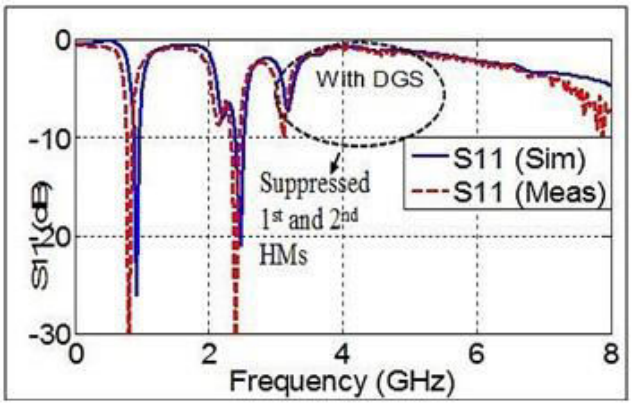

Figure-5. Simulated and measured S11 for the antenna with DGSs.

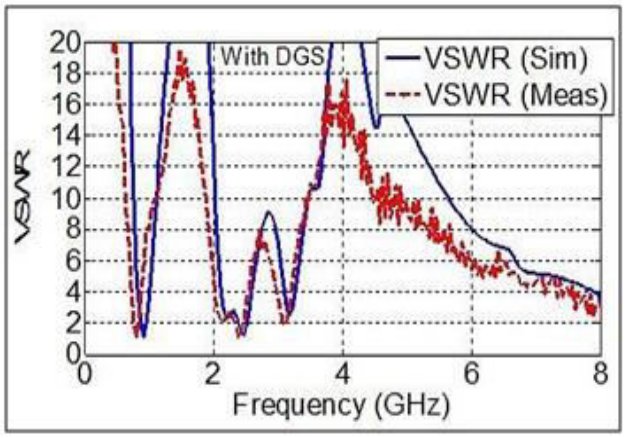

Figure-6. Simulated and measured VSWRs for the antenna with DGSs.

Performance comparison of the antennas with and without DGSs

Figure-7 compares the measured return losses (S11) of the proposed antennas with and without DGSs. After applying the DGS technique, the antenna only operates within the two desired frequencies with improved performance. The return loss for the first and second operating frequencies increases to –25.5 and –20.5 dB, respectively. Application of the DGSs eliminates the third undesired frequency. The DGS technique effectively suppresses unwanted frequencies (3.6 and 4.7 GHz) by reducing their amplitudes. Table-2 shows the recorded data difference between the simulated and measured return losses of the antennas at both desired and undesired frequencies.

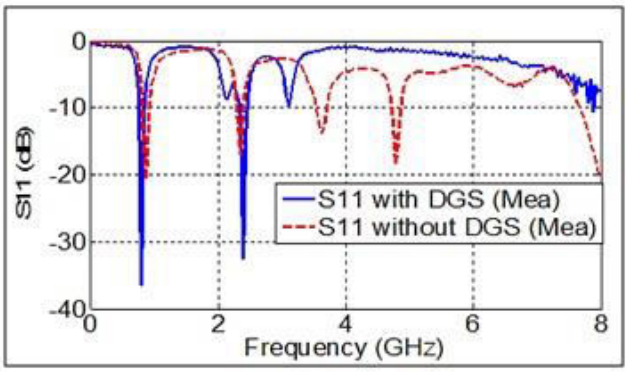

Figure-7. Measured S11 of antennas with and without DGSs.

Table-2. Differences between the simulated and measured S11 of the proposed antenna.

fr (GHz)	Simulated S11(dB)		Measured S11(dB)	
	Without DGS	With DGS	Without DGS	With DGS
0.9	-14.64	-26.04	-36.2	-36.39
2.4	-18.82	-21.01	-32.4	-32.55
3.6	-14.44	-3.7	-13.8	-8.5
4.7	-18.24	-2.3	-18.3	-1.06

Figure-8 presents a comparison of the measured VSWRs of the proposed antennas with and without DGSs. The figure clearly illustrates the effect of the DGSs on the third and fourth frequencies. Thus, the designed antenna only operates at the two desired frequencies.

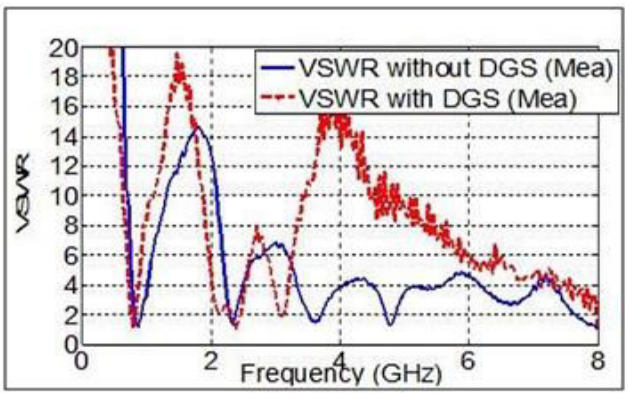

Figure-8. Measured VSWRs of antenna with and without DGSs.

According to Figure-9, the simulated gain before the DGSs was applied at all frequencies studied is above 1 dB. Application of the DGSs affects the harmonic frequency gain. Thus, the designed antenna operates at dual band frequencies. The proposed antenna is fabricated on the selected dielectric substrate, as shown in Figure-10.

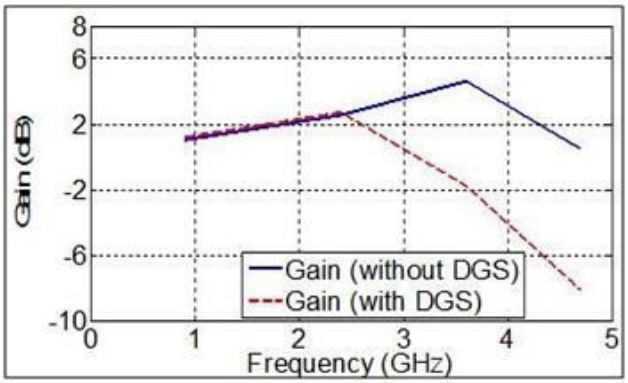

Figure-9. Simulated antenna gain performance with and without DGSs.

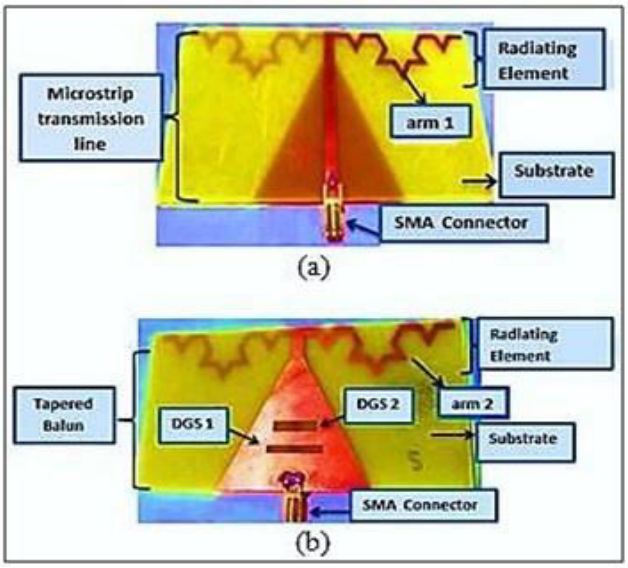

Figure-10. Fabricated inverted Koch fractal dipole antennas (a) without DGSs and (b) with DGSs

PARAMETRIC STUDY AND ANALYSIS

Parametric studies were conducted based on return loss results obtained from various DGS widths and positions. The influence of the rectangular DGS1 width is shown in Figure-11. The slot length (L5) was kept constant at 16 mm in all cases, and the etched slot width (W4) was varied.

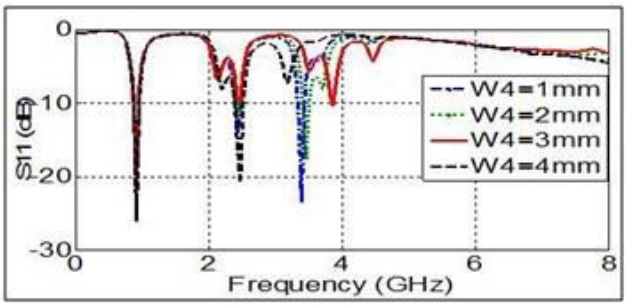

Figure-11. Simulated S11 for the proposed antenna with different DGS1 slot widths.

Table-3. Effects of a rectangular DGS1 with different widths and positions on antenna return loss.

DGS Dimensions (mm)		DGS1 Location (mm)		Return loss (dB)		
Length	Width	V_{min}	V_{max}	f1	f2	f3
21	1	10	11	-17.9	-18.5	-10.7
21	2	20	22	-14.6	-21.8	-15.5
21	3	10	13	-19.4	-20.2	-2.77
21	4	8	12	-22.9	-3.53	-3.17

Table-3 shows how the width and location of DGS1 affect the return losses of the operating frequencies as well as undesired harmonic frequencies. The best result is obtained when W4 is 4 mm, Vmin is 20 mm, and Vmax is 24 mm. In this case, the capability of DGS1 to eliminate undesirable frequencies is optimized. DGS1 clearly increases S11 at both operating frequencies in comparison with the conventional design.

The effect of the etched slot width of the rectangular DGS2 is shown in Figure-12. The slot length (L6) was kept constant at 21 mm for all cases studied, and the etched slot width (W5) was varied. Table-4 illustrates the effects of the width and location of DGS2 on the return losses of the operating frequencies as well as undesired harmonic frequencies. The best result is obtained when W5 is 3 mm, Vmin is 10 mm, and Vmax is 13 mm. Hence, the capability of DGS2 to eliminate undesired frequencies is optimized. S11 performance shows clear improvements at both operating frequencies in comparison with the conventional design.

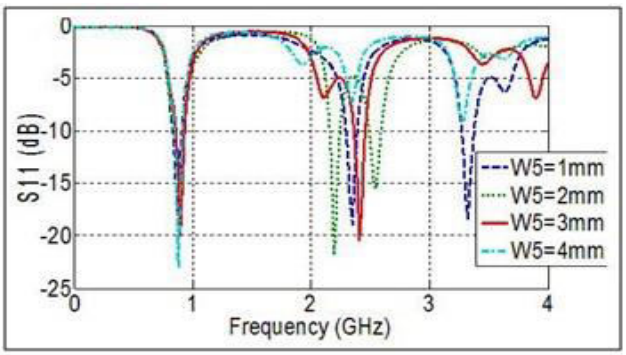

Figure-12. Simulated S11 for the proposed antenna with different DGS2 slot widths.

Table- 4. Effects of a rectangular DGS2 with different widths and positions on antenna return loss (S11).

DGS Dimensions (mm)		DGS1 Location (mm)		Return loss (dB)			
L	W	V_{min}	V_{max}	f1	f2	f3	f4
16	1	20	21	-19.6	-13.7	-23.4	-1.1
16	2	15	17	-20.9	-11.6	-3.5	-1.2
16	3	16	19	-21.7	-9.9	-3.6	-1.4
16	4	20	24	-25.5	-20..4	-1.6	-1.0

The calculated bandwidths of the resonant frequencies with and without DGSs are summarized in Table-5 .It can be observed that, how much is the bandwidth of the operating frequencies improved after DGSs were applied.

Table-5. Simulated bandwidth with and without DGSs.

Frequency	Bandwidth Without DGSs	Bandwidth With DGSs
(GHz)	BW%	BW%
0.9	11.5	12.75
2.4	5.356	6.414
3.6	4.018	-
4.7	3.696	-

Figure-13 shows the magnitude of the surface current distribution of the proposed antenna. The red color field indicates large values, whereas the blue color field refers to small values of the current. At 0.9 and 2.4 GHz, the current is nearly entirely distributed over the Koch fractal dipole arms. At 3.6 and 4.7 GHz, significant differences compared with the two previous cases may be observed. The highest current distribution is observed at the corner of the DGS slot. Thus, the current follows the curvature of the DGS slot. Because frequency increases, the current follows a curved path rather than a straight one.

To achieve the desired radiation pattern, the surface current must be controlled. Application of DGSs would be very useful to control the path of the surface current.

Figure-14 shows the simulated and measured E-plane (y-z plane) and H-plane (x-z plane) radiation patterns of the antenna. The obtained overall radiation patterns of both planes are nearly omni-directional, which is required for wireless communication applications. Moreover, the radiation pattern of the antenna exhibits good symmetry between the E and H- planes.

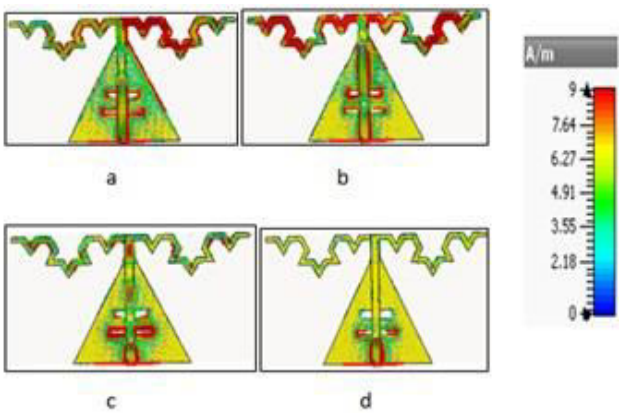

Figure-13. Effect of DGS on the surface current distribution of the antenna: (a) At 0.9 GHz, (b) at 2.4 GHz, (c) at 3.6 GHz, and (d) at 4.7 GHz.

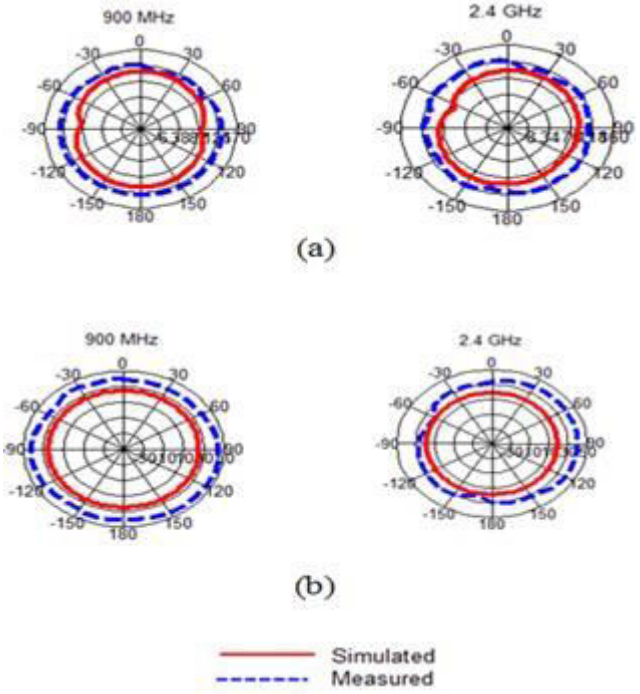

Figure-14. Measured and simulated radiation patterns: (a) The E-plane (XZ-plane) and (b) the H-plane (YZ-plane).

CONCLUSIONS

A dual band fractal dipole antenna was designed and evaluated. To suppress undesired higher-order harmonics, two DGSs were loaded on the triangular tapered balun. An extensive parametric study was carried out to examine antenna performance and capability. The DGS dimensions and positions on the tapered balun were optimized to achieve the desired antenna operation and characteristics and suppress undesirable harmonics. The results obtained demonstrate that the antenna exhibits good performance in terms of return loss, voltage standing wave ratio (VSWR), gain, and radiation patterns.

ACKNOWLEDGEMENTS

The authors would like to thank University Tun Hussein Onn Malaysia (UTHM) and Al-Zaytoonah University of Libya for supporting this project as well as all other parties who have directly or indirectly contributed to the success of this work. The technical support provided by the Center for Applied Electromagnetics in UTHM is highly appreciated.

REFERENCES

[1] S. Emanoil, D. Iancu, J. Glossner. 2006. Modified printed dipole antennas for wireless multi-band communication systems. U.S. Patent No. 7,034,769.25.

[2] C. A. Balanis. 2011. Modern antenna handbook.U.S. Patent No. 7,095,382.

[3] J. M. Steyn, W. J. Odendaal, J. Joubert. 2009. Dual-band dual polarized array of WLAN applications. Progress in Electromagnetics Research C. 151-161.

[4] K. Fujimoto, H. Morishita. 2014. Modern small Antennas. Cambridge university press.

[5] M. Z. A. Karim, M. K. A. Rahim, T. Masri. 2009. Fractal Koch dipole antenna for UHF band application. Microwave and Optical Technology Letters. 51(11): 2612-2614.

[6] H. Zhang, H. Xin H. 2009. A dual band dipole antenna with integrated balun. IEEE transactions on Antennas and Propagation. 57(3): 786-789.

[7] A. Reha, A. El-Amri, O. Benhmammouch, A. O. Said. 2014. Fractal Antennas: A Novel Miniaturization Technique for wireless networks. Transactions on Networks and Communications. 2(5): 165-193.

[8] M. Joseph, R. K. Raj, M. N. Suma, C. K. Aanandan, K. Vasudevan, P. Mohanan. 2007. Microstrip-fed Dual band Folded Dipole Antenna for DCS/PCS/2.4GHz WLAN Applications. International Journal for Wireless and Optical communications (IJWOC). 4(1): 43-51.

[9] A. Mirkamali, P. S. Hall, M. Soleimani. 2006. Reconfigurable printed-dipole antenna with harmonic trap for wideband applications. Microwave and optical technology letters. 48(5): 927-929.

[10] S. A. Hamzah, M. Esa, N .N. N. Abd Malik, M. K. H., Ismail. 2010. Reduced Size Harmonic Suppressed Fractal Dipole Antenna with Integrated Reconfigurable Feature. IEEE 6th International Conference on Signal-Image Technology and Internet Based Systems. pp. 149-152.

[11] K. Payandehjoo, R. Abhari. 2008. Suppression of Unwanted Harmonics Using Integrated Complementary Split-Ring Resonators in Nonlinear Transmission Line Frequency Multipliers. IEEE Transactions on Microwave Theory and Techniques. 56(4): 931-941.